Langmuir

Article

pubs.acs.org/Langmuir

Simple Ligand Exchange Reactions Enabling Excellent Dispersibility and Stability of Magnetic Nanoparticles in Polar Organic, Aromatic, and Protic Solvents

Xinyu Wang,[†] Richard D. Tilley,[‡] and James J. Watkins*[,†]

[†]Polymer Science and Engineering Department, University of Massachusetts Amherst, 120 Governors Drive, Amherst, Massachusetts 01003, United States

[‡]MacDiarmid Institute, Victoria University of Wellington, Wellington, New Zealand

Supporting Information

ABSTRACT: The use of magnetic nanoparticles (MNPs) in real-world applications is often limited by the lack of stable solutions of monodisperse NPs in appropriate solvents. We report a facile one-pot ligand exchange reaction that is fast, efficient, and thorough for the synthesis of hydrophilic MNPs that are readily dispersed in polar organic and protic solvents (polarity index = 3.9−7.2) including alcohols, THF, DMF, and DMSO for years without precipitation. We emphasize the rational selection of small-molecule ligands such as 4-hydroxybenzoic acid (HBA), 3-(4-hydroxyphenyl)propionic acid (HPP), and gallic acid (GAL) that provide strong bonding with the MNP (FePt and FeO_x) surfaces, hydrophilic termini to match the polarity of target solvents, and offer the potential for hydrogen-bonding interactions to facilitate incorporation into polymers and other media. Areal ligand densities (Σ) calculated based on the NP core size from transmission electron microscopy (TEM) images, and the inorganic fractions of NPs derived from thermogravimetric analysis (TGA) indicated a significant (2−4 times) increase in the ligand coverage after the exchange reactions. Fourier transform infrared spectrometry (FTIR) and ^{1}H nuclear magnetic resonance (NMR) studies also confirmed anchoring of carboxyl groups on NP surfaces. In addition, we demonstrate a facile one-step in situ synthesis of FePt NPs with aromatic ligands for better dispersibility in solvents of intermediate polarity (polarity index = 1.0−3.5) such as toluene, chlorobenzene, and dichloromethane. The creation of stable dispersions of NPs in solvents across the polarity spectrum opens up new applications and new processing widows for creating NP composites in a variety of host materials.

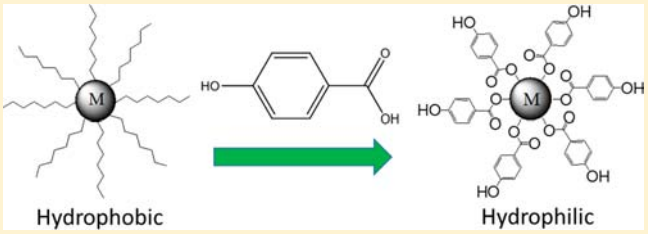

INTRODUCTION

Because of their unique size- and shape-dependent properties, magnetic nanoparticles (MNPs) have been widely utilized in a variety of fields including contrast enhancement in magnetic resonance imaging (MRI),[1−4] magnetic field assisted transport and separation of biological entities,[5−9] biomedicine,[10−12] magnetic-triggered drug delivery,[5,6,13] hyperthermia for cancer therapy,[14] ultrahigh-density magnetic storage media,[15,16] exchange-coupled nanocomposite magnets,[17] and inorganic−organic hybrid metamaterials.[18,19] Each of these applications requires monodisperse MNPs that are stably dispersed in solvents of different polarities, a necessity which is not usually satisfied by conventional synthetic routes using alkyl capping agents. Currently, population of magnetic nanocrystals capped with lengthy aliphatic ligands from organic-phase synthesis can be relatively monodisperse, but they are only stable in nonpolar solvents. In contrast, MNPs that are prepared using conventional water-phase synthetic protocols often yield nanocrystals with high distributions of particle size, crystalline anisotropy, and magnetism. The resulting polydisperse nanocrystals result in reduced performance in areas such as magnetic imaging.

As a result, great efforts have been made recently toward the preparation of monodisperse MNPs that can be dispersed and are stable in other solvents, especially aqueous solutions for biological applications. To date, a number of research groups have exploited various tools to stabilize the MNPs in solutions, such as using water-soluble small-molecule or polymeric protective ligands to bond with the NPs, creating an electrostatic double layer on the NP surface,[20,21] and building a NP core−shell structure to reduce interparticle surface interactions or to provide alternative anchoring groups for better bonding between the NPs and ligands.[22,23] Polymeric ligands[24−30] or bulky bio-based molecules[31,32] are often employed (via in situ syntheses or ligand exchange reactions) for the syntheses of such MNPs due to their greater number of anchoring groups or multiple types of ligand functionality[33] within a single molecule. In addition, MNPs made with longer or bulkier ligands are generally more resistant to large scale agglomeration. However, ligands containing more bonding sites

Received: December 11, 2013
Revised: January 17, 2014
Published: January 24, 2014

often result in bridging between NPs, which is even more significant as the ligand chain length extends. Moreover, polymeric ligands usually require tedious and NP-specific synthetic efforts in order to obtain desired functionality and structural design. Lastly, the large corona created by the lengthy ligands will effectively reduce the inorganic fraction of the MNPs, leading to the abatement of the proposed physical properties (magnetism in this case) stems from the inorganic core in the design of MNP-doped hybrid materials.

On the other hand, the utility of small-molecule ligands has been widely studied. Generally such methods usually involve the substitution of the native ligands with short hydrophilic ligands based on the synthetic routes already well-developed for alkyl-functionalized iron oxides (Fe_2O_3 or Fe_3O_4),[34−36] cobalt ferrite ($CoFe_2O_4$),[37] manganese ferrite ($MnFe_2O_4$),[37,38] iron platinum (FePt),[15,39,40] and Ni/NiO.[41−43] Although the use of thiols[44,45] and silanes[46] have been reported, most studies focus on hydrophilic ligands bearing carboxyl groups or amines such as nitrilotriacetic acid (NTA),[47] dimercaptosuccinic acid (DMSA),[2−4,48]3,4-dihydroxyhydrocinnamic acid (DHCA),[49] dopamine,[50−52] imidazole,[7] and their derivatives due to the high affinity of these groups for the MNP surfaces. The obvious merits of these methods include the relatively low size distribution inherited from the as-synthesized hydrophobic NPs, little or no synthetic efforts for the ligands, and relatively high inorganic fraction in the NPs. However, the trade-offs also cannot be neglected. First, the ligand stabilization is frequently not as good as that found with polymeric ligands. Further, the issue of bridging between particles is not completely solved since most of these short ligands still have multiple anchoring groups, leading to the agglomeration of NPs in solution and the formation of bigger clusters (some with fair stability). More recently, researchers from Murray's[53] and Helms's[54] groups have reported a more generalized two-step ligand-exchange reactions involving the initial stripping of the native ligands with nitrosonium tetrafluoroborate ($NOBF_4$) or trialkyloxonium salts (Meerwein's salt) and subsequent addition of desired protecting ligands. These methods have proven to be effective and could be applied to some magnetic NPs as well.

While existing literature provides a number of options for many solvent systems, there are few available for use in the midrange of the solvent polarity spectrum. In this report, we demonstrate a fast, thorough, and one-step ligand-exchange reaction for the preparation of hydrophilic NPs that can be readily dispersed in polar organic solvents with superior stability for years. We focus on the rational design and choice of small-molecule ligands which will provide not only sufficient protection against particle agglomeration but also the ability to be dispersed in solvents with a wide range of polarities (polarity index = 3.9−7.2). The chosen ligands are equipped with functional groups that are capable of secondary interactions such as hydrogen bonding with target media including the solvent or subsequent hosts for NP composites. We further show the generality of this method, such that it can be applied to many magnetic NP species regardless of their size and shapes. Finally, to complete the polarity spectrum, we demonstrate the in situ synthesis of aromatically functionalized FePt NPs that can be readily dispersed in aromatic solvents with intermediate polarities (polarity index = 1.0−3.5). The synthetic strategies reported here will open a door for magnetic NPs to be utilized in a wider range of applications in which NP dispersions in polar organic or aromatic solvents were required.

EXPERIMENTAL SECTION

Materials. 4-Hydroxybenzoic acid (99%), 3-(4-hydroxyphenyl)-propionic acid (98%), gallic acid (98%), citric acid (reagent ACS, 99.5%), oleylamine (approximate C18-content 80−90%), and oleic acid (97%) were purchased from Acros Organics. Dioctyl ether (99%), iron(0) pentacarbonyl (>99.99%, trace metals basis), platinum(II) acetylacetonate (97%), iron(II) acetylacetonate (99.95%, trace metals basis), trioctylphosphine (97%), biphenyl-4-carboxylic acid (95%), and 2-naphthoic acid (98%) were purchased from Sigma-Aldrich. 1,2-Hexadecanediol (>98%) was purchased from TCI America, and carboxyl-terminated polystyrene (1K Da) was purchased from Polymer Source. Common solvents were purchased from Fisher Scientific. All reagents were used as received without further purification.

Hydrophobic FePt Nanoparticle Synthesis. The synthesis of hydrophobic FePt NPs was based on the method previously reported by Sun et al.[15] In a typical synthesis, platinum(II) acetylacetonate (197 mg, 0.5 mmol), 1,2-hexadecanediol (390 mg, 1.5 mmol), and dioctyl ether (20 mL) were first loaded into a three-necked round-bottom flask and stirred using a magnetic stirring bar. The mixture was heated to 100 °C under a gentle flow of N_2 to remove oxygen and moisture. Oleic acid (0.16 mL, 0.5 mmol) and oleylamine (0.17 mL, 0.5 mmol) were introduced to the mixture and equilibrated for 10 min before iron(0) pentacarbonyl (0.13 mL, 1 mmol) was injected. For the synthesis of 2 nm FePt NPs, trioctylphosphine (0.22 mL, 0.5 mmol) was introduced as a third protecting ligand. The mixture was then heated to reflux at 297 °C for 30 min (ramp rate as a variable, 5−15 °C/min). The reaction was stopped by removing the heat source and allowed to cool naturally to room temperature. The resulting NPs were collected by centrifugation using ethanol as the antisolvent. Particles were typically washed with hexanes and ethanol 2−3 times to remove excessive ligands. The as-synthesized hydrophobic NPs could be readily dispersed in solvents with low polarity such as alkanes, 1-alkenes, and chlorinated solvents.

Hydrophobic Iron Oxide Nanoparticle Synthesis. The synthesis of iron oxide (FeO_x) NPs was based on the modification of Park's method for Ni and NiO NPs.[42] Iron(II) acetylacetonate (0.26 g), oleylamine (1 mL), and trioctylphosphine (5 mL) were combined in a three-necked round-bottom flask followed by the complete removal of residue oxygen with the freeze−pump−thaw technique. The reaction was heated to 100 °C under the protection of N_2 and equilibrated for 10 min to ensure the even distribution of reagents. The reactor was then brought to 200 °C for 30 min. The collection and purification procedures of these NPs are similar to that of hydrophobic FePt NPs.

One-Step Ligand Exchange Reaction for Hydrophilic MNPs. A typical reaction begins with the mixing of 50 mg of hydrophobic NP powder and 500 mg of hydrophilic ligand with 20 mL of solvent (ethanol, methanol, tetrahydrofuran, or *N*,*N*-dimethylformamide) in a scintillation vial. To promote the ligand exchange reaction, 10 min of sonication and subsequent stirring were performed to ensure a satisfying conversion rate. The solution became dark yet transparent within a few minutes, indicating the thorough dispersion of NPs in the polar solvents. The exchanged NPs were precipitated with the addition of excessive hexanes as the antisolvent and collected by centrifugation at 5K rpm for 5 min. The resulting NPs were washed with ethanol/hexanes combination for 2 or 3 times to remove any excessive ligands. The resulting hydrophilic NPs showed satisfactory dispersibility in solvents such as ethanol, methanol, 2-propanol, tetrahydrofuran, or *N*,*N*-dimethylformamide and remained quite stable during the period of observation (over a year). See Figures S3−S5 for photos of stable MNP dispersions. The ligand exchange reaction could also be carried out by a two-phase method in which hydrophobic NPs were extracted completely from the hydrophobic hexanes phase to the polar *N*,*N*-dimethylformamide phase. This reaction was facilitated by gentle stirring for about 1 h.

In Situ Synthesis of FePt Nanoparticles with Aromatic Ligands. The procedures for synthesis and purification are similar to the synthesis of hydrophobic FePt NPs with the differences that

aromatic ligands (biphenyl-4-carboxylic acid, 2-naphthoic acid, or polystyrene, 1 mmol) were added prior to heating, and the reaction mixture was kept at 100 °C for a longer time (20 min) until ligands were completely dissolved. The resulting NPs could be best dispersed in toluene, chloroform, chlorobenzene, and tetrahydrofuran.

Characterization. Transmission electron microscopy (TEM) samples were prepared by drop-casting diluted NP suspension onto 400 mesh carbon-supported copper grids to be examined with a JEOL 2000FX II TEM operating at 200 kV. Image analysis of the TEM images was performed with ImageJ software for the average core size of NPs. At least 500 particles were measured for each NP species to ensure that an accurate number was obtained. Dynamic light scattering (DLS) was done with a Malvern Zetasizer Nano ZS to obtain the average hydrodynamic diameter of NPs in their dispersants. Fourier transform infrared spectroscopy (FTIR) spectra were taken with a PerkinElmer Spectrum 100 FT-IR spectrometer. Samples were drop-casted from NP suspensions onto KBr pellets and measured with transmission mode for better signal-to-noise ratio. Thermogravimetric analysis (TGA) data were performed with a TA Instruments Q500 thermogravimetric analyzer with a ramping rate of 15 °C/min under a constant purging with air of 60 mL/min. 10−20 mg of NPs was used for each measurement. ^{1}H nuclear magnetic resonance (NMR) was performed on a Bruker DPX300 NMR using chloroform-*d* and dimethyl-d_6 sulfoxide as the solvents.

RESULTS AND DISCUSSION

Selection of Small-Molecule Ligands and the Reaction Scheme. The manipulation of NP's solubility in organic solvents could be achieved by the rational choice of the protecting ligands. For an ideal ligand candidate, we used commercially available small-molecule ligands for convenience and low cost. The ligands were short to reduce the amount of organic content of the NP, yet enough to provide sufficient protection against particle agglomeration. Instead of choosing ligands with extended alkyl chains, we took advantage of bulky phenyl rings, which provided sufficient steric hindrance to prevent the inorganic cores from agglomerating. The ligands had one bonding site that strongly coordinate with the NP surface to provide particle stability so that the original ligand would leave; however, the number of anchoring groups on each ligand was also limited to prevent bridging between individual particles. Last but not the least, we chose ligands with hydrophilic functional termini, which provide MNPs with good solubility in polar solvents and could serve as potential H-bonding sites.

Scheme 1 shows the ligand exchange strategy we have taken and ligand candidates we have chosen to enable the magnetic NPs to be well dispersed in polar solvents. Based on the criteria mentioned above, 4-hydroxybenzoic acid (HBA), 3-(4-hydroxyphenyl)propionic acid (HPP), and gallic acid (GAL) were proven to be the ideal candidates for promising ligand exchange reactions. They all have the similar structure that one carboxyl group and some hydroxyl groups (n = 1, 3) are positioned at the two ends of the molecules, sharing a benzene ring in the middle. Such configuration satisfies our proposed condition that the ligand length is very short yet bulky enough to form a ligand monolayer on the NP surface that screens undesired interparticle interactions. Take 4-hydroxybenzoic acid for example; the exchanged NP has carboxyl groups anchoring to the NP surface, bulky phenyl groups forming a passivating monolayer, and hydroxyl group pointing out for favorable interaction with polar solvents.

Exchanged 4 nm Hydrophilic FePt Nanoparticles. FePt NPs with an average diameter of 4 nm were first used to make hydrophilic NP. Figure 1 shows the transmission electron microscopy (TEM) images of the 4 nm FePt NPs before and after the ligand exchange. The alkyl-functionalized NPs (FePt-alkyl) were dispersed in hexanes whereas the hydrophilic NPs (FePt-OH) were dispersed in DMF. NP suspensions were

Scheme 1. Proposed Illustration of One-Step Ligand Exchange Reaction, Ligand Candidates, and the Target Solvents

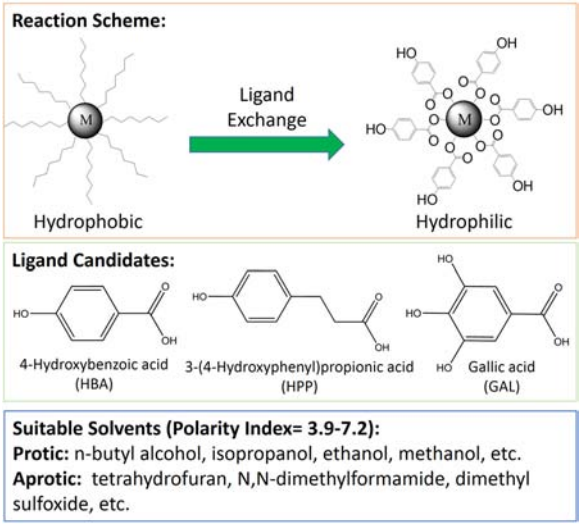

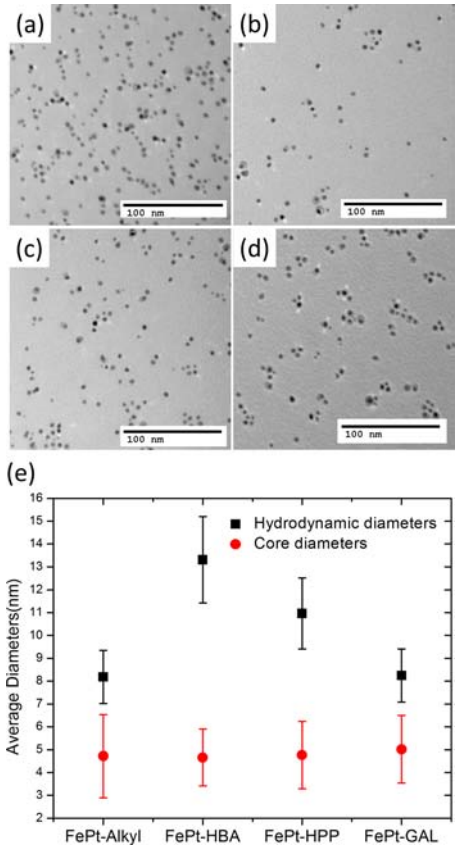

Figure 1. Transmission electron microscopy (TEM) images of (a) as-synthesized hydrophobic FePt NPs, (b) FePt NPs with 4-hydroxybenzoic acid (HBA), (c) FePt NPs with 3-(4-hydroxyphenyl)-propionic acid (HPP), and (d) FePt NPs with gallic acid (GAL). (e) Average hydrodynamic diameters of NPs obtained from Zetasizer (DLS) and core diameters from image analysis of TEM images.

dx.doi.org/10.1021/la404757q | Langmuir 2014, 30, 1514−1521

drop-casted on carbon-supported copper grids and examined after the solvents have completely evaporated. The FePt NP with native ligands were very well dispersed in nonpolar solvents such as hexanes as reported previously by a number of researchers. It is clear that all the FePt-OH NPs were dispersed equally well compared with FePt-alkyl NPs (Figure 1b–d). No bridging or agglomeration was found in the TEM images after the new ligands were attached nor was there any change in the size and shape of the nanocrystals. The fact that the average core size and hydrodynamic diameters of FePt NPs have remained relatively consistent before and after the ligand exchange also confirms our conclusion from the TEM images. Noticed that the hydrodynamic diameters of the NPs obtained with the Malvern Zetasizer (Nano ZS) are somewhat larger than the core size. One reason is that the light was also diffracted by the solvents captured by the extended ligands in the solution so the hydrodynamic diameters appeared to be larger than the actual values. The second reason is that the sizes of the particles were close to the instrument's limitation such that biased readings were obtained. Regardless of that, all the exchanged FePt NPs show only unimodal light scattering peaks, ruling out the presence of any particle aggregation in the dispersion (Figure S1).

Fourier transform infrared spectroscopy (FTIR) was performed to map the ligand structures on the NP surface as shown in Figure 2. The characteristic peaks representing the

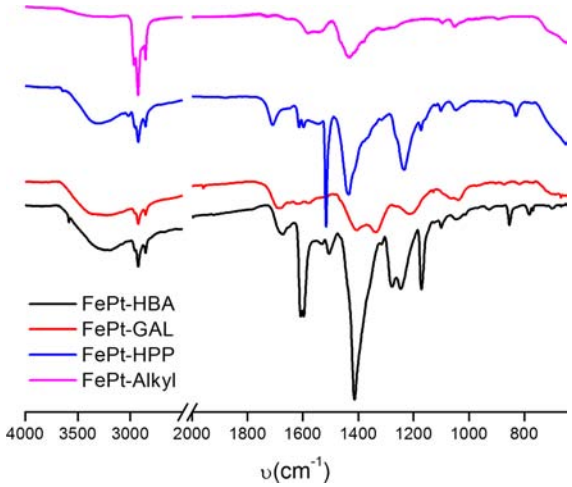

Figure 2. Fourier transform infrared spectroscopy (FTIR) spectra of FePt NPs.

C–H stretching at 2800–3000 cm^{-1} from oleic acid and oleylamine of FePt-alkyl NPs were significantly reduced after the exchange reaction, representing the removal of native ligands. However, since the C–H stretching peaks on the phenyl groups of the hydrophilic ligands are found in the same range, it was difficult to quantify the actual amount of ligands been replaced. The presence of phenyl groups was also confirmed by the group of four peaks between 1450 and 1600 cm^{-1} from the backbone stretching of benzene rings as well as the single sharp peaks at 800–900 cm^{-1} from the nonplanar wagging and twisting of C–H bonds. For all the hydrophilic NPs, we have observed a strong but wide peak in 3100–3400 cm^{-1} which is characteristic of O–H stretching from the highly hydrogen-bonded hydroxyl groups on phenyl rings. The single peaks at 1680–1710 cm^{-1} are very indicative of the presence of C=O in-plane stretching vibrations, suggesting the anchoring of carboxyl groups on NP surfaces. As for the strong peaks at near 1400 cm^{-1}, we believe that it was the characteristic peaks of the FePt NPs since it was shown for all NP species. In summary, the FTIR spectra of MNPs revealed that the hydrophilic ligands have indeed replaced the majority of the native ligands on the MNPs.

Thermogravimetric analysis (TGA) was performed to determine the ligand coverage of the FePt NPs (Figure 3).

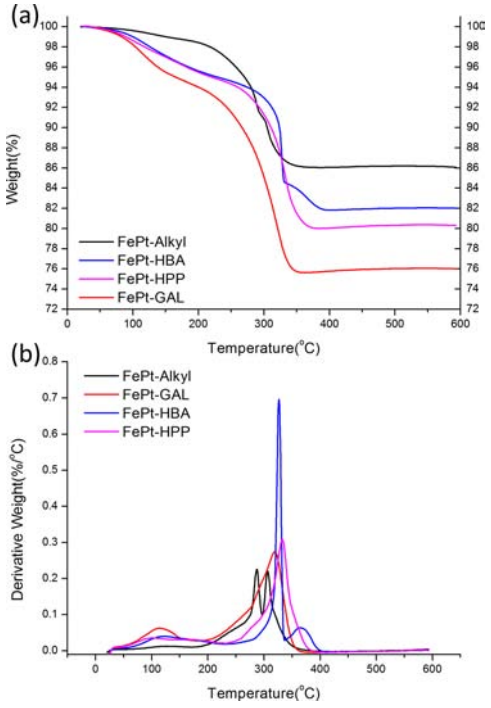

Figure 3. (a) Thermogravimetric analysis (TGA) of FePt NPs and (b) the rate of weight loss as temperature increases.

The samples were thoroughly purified to remove all the excessive ligands by the centrifugation method. We have observed that the ligand fraction of FePt–OH NPs (18% for HBA, 20% for HPP, and 24% for GAL) exceeded that of FePt-alkyl NPs (14%). From the slope of the TGA curves we have obtained the rate of weight loss with respect to temperature ramping, showing that the hydrophilic ligands were pyrolyzed at a higher temperatures. The relatively unimodal peaks of the leaving groups for FePt–OH NPs (as opposed to the bimodal peaks given by the native oleic acid and oleylamine) suggest that there was little or no native ligand left and the ligand exchange reaction was thorough. On the basis of the average core size and TGA data shown above and assuming that the density of NPs is identical with that of their bulk state regardless of particle size, we were able to calculate the areal ligand coverage (Σ) as shown in Figure 4. FePt-alkyl NPs had an areal density of Σ = 4.2 ligands/nm^2, assuming a 50:50 mixture of oleic acid and oleylamine. In comparison, the areal ligand densities for FePt–OH NPs are Σ = 11.3 ligands/nm^2 with HBA, Σ = 10.7 ligands/nm^2 with HPP, and Σ = 14.16 ligands/nm^2 with GAL. These data suggest that the average number of ligands on a NP surface have increased for 2–4 times after the ligand exchange reaction thanks to the small, rigid structure of the hydrophilic ligands. The enrichment of ligands on NP surface provides superior stability of these

dx.doi.org/10.1021/la404757q | Langmuir 2014, 30, 1514–1521

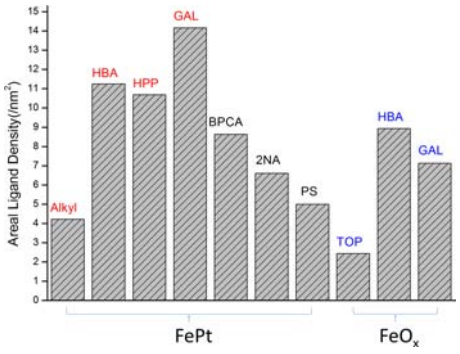

Figure 4. Areal ligand density (Σ) of NPs calculated from image analysis and thermogravimetric (TGA) data.

hydrophilic NPs in polar organic solvents. (For detailed calculations please refer to the Supporting Information.)

Ligand Exchange Reactions for MNPs of Various Sizes and Nature. This method for ligand exchange could also be applied to FePt NPs with different sizes. TEM images of FePt-OH NPs from 2 to 12 nm are shown in Figure 5. All the ligand

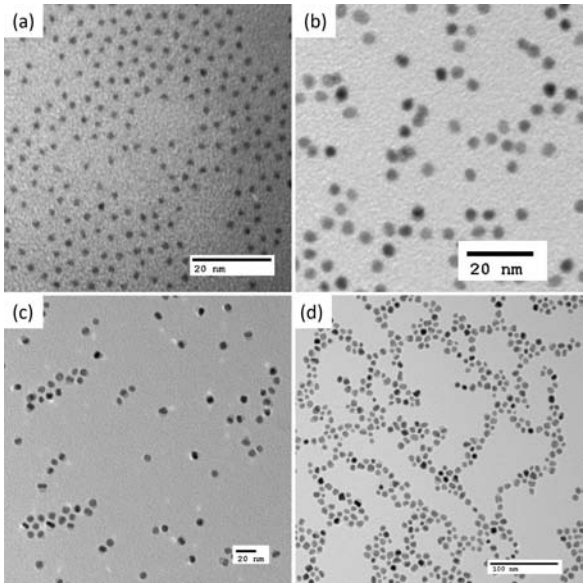

Figure 5. Transmission electron microscopy (TEM) images of exchanged hydrophilic FePt NPs showing average diameters of (a) 2, (b) 4, (c) 8, and (d) 12 nm.

exchange reactions were successful regardless of the size and shape of the particles. Interestingly, we have found that the cubic-like 8 and 12 nm NPs were both successfully exchanged (Figure 5c,d). However, it is worth noting that if the size of the particle is larger than 8 nm, the solution stability of hydrophilic NPs with ligands that has only one hydroxyl group (such as 4-hydroxybenzoic acid) appears to be not as ideal as for smaller NPs. The dispersion of such NPs will begin to precipitate out on vial walls in 24 h and became totally settled after a few weeks. The use of ligands with multiple hydroxyl groups such as gallic acid overcomes the problem nicely. As a result, we have not observed significant precipitation of 12 nm FePt NPs decorated with gallic acid during long-time observation. This result is very compelling since the use of long-chain ligands or polymeric ligands was usually a necessity to prevent large magnetic NPs from collapsing with each other. The utilization of just small ligands dramatically increases the inorganic fraction of the NPs, providing better opportunities for high-performance organic/inorganic hybrid materials in the sense that larger effective volume fractions of "functional" inorganic materials could be incorporated into the organic matrix.

When the core size of NPs is reduced to less than 2 nm, the magnetization of superparamagnetic FePt NPs induced by strong magnetic field is relatively low so that it is possible to examine the ligand bonding with regular proton nuclear magnetic resonance (^{1}H NMR). The proton NMR of FePt-HBA NPs confirmed the existence of 4-hydroxybenozic acid on NPs. Figure 6a shows that the peak at 5.4 ppm representing the

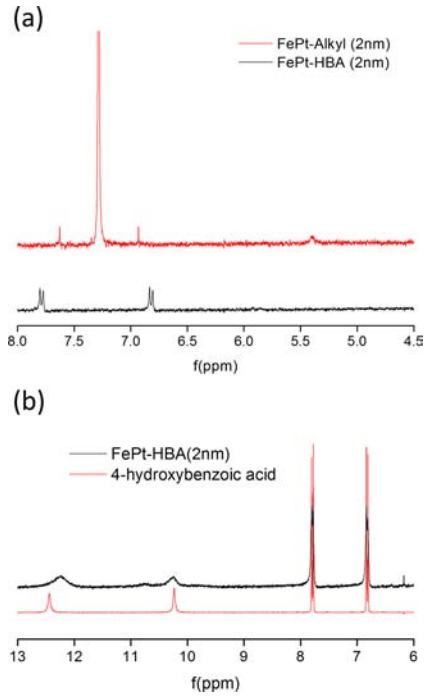

Figure 6. Proton nuclear magnetic resonance (^{1}H NMR) spectra of the 2 nm superparamagnetic FePt NPs and the corresponding ligand.

protons on the double bond of the oleic acid and oleylamine has completely disappeared after the ligand exchange, indicating a total removal of the alkyl ligands. TGA of the NPs is also in good agreement of this finding (Figure S6). Also, we have observed a 0.2 ppm shift for the protons on the carboxyl group from 12.4 to 12.2 ppm comparing the free HBA ligand and the NP decorated with HBA as shown in Figure 6b. This shift means that the O−H bond length of the carboxyl groups of HBA on NPs was different from its free and relaxed state. It is the direct proof that the carboxyl groups were coordinating with the inorganic surface. It is also worth noting that the native alkyl-functionalized 2 nm FePt tends to precipitate out in 24 h due to their large surface areas, whereas the exchanged NPs remains stable for at least a year. This is another evidence of the superior stability of NP dispersions brought by the chosen ligands.

These ligands were also used to functionalize iron oxide NPs and have achieved similar results as the FePt NPs. The as-synthesized FeO_x NPs was fairly monodisperse with an average diameter of 5 nms (Figure 7a) and was protected with trioctylphosphine (TOP), a better leaving group than oleic acid and oleylamine. TEM images (Figure 7b,c) and DLS (Figure 7d and Figure S2) data showed that the exchanged NPs were

dx.doi.org/10.1021/la404757q | Langmuir 2014, 30, 1514−1521

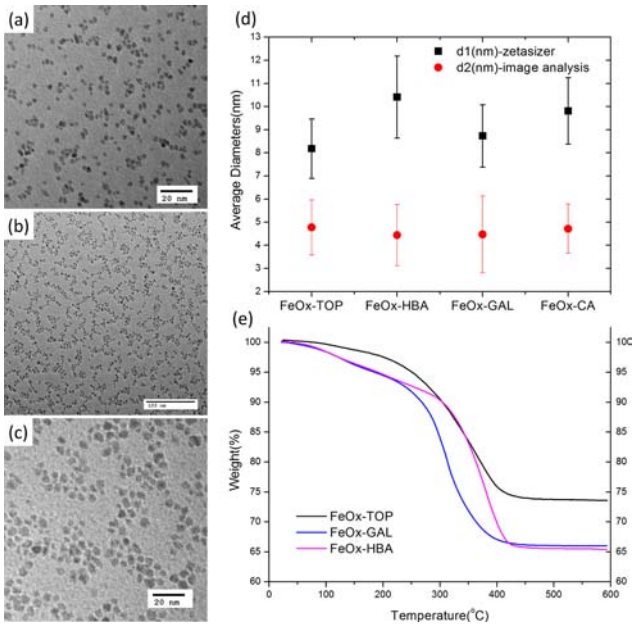

Figure 7. Transmission electron microscopy (TEM) images of FeO_x NPs with (a) trioctylphosphine (TOP), (b) 4-hydroxybenzoic acid (HBA), and (c) gallic acid (GAL) as ligands. (d) Average diameters of NPs obtained from Zetasizer (DLS) and image analysis. (e) Thermogravimetric analysis (TGA) of the NPs.

well-dispersed in organic solvents, and their core size as well as hydrodynamic diameter remains unchanged. Figure 7e shows that the ligand fractions have increased after the ligand exchange and the hydrophilic ligands have completely replaced trioctylphosphine. The areal ligand coverage (Σ) of hydrophilic iron oxide NPs in Figure 4 shows an even more significant elevation in the number of ligands on the exchanged iron oxide NPs (Σ = 8.9 ligands/nm^2 for HBA and Σ = 7.1 ligands/nm^2 for GAL) compared with the native FeO_x-TOP (Σ = 2.4 ligands/nm^2). In addition, we expect that this method could also be applied to MNPs of other natures such as nickel oxide, cobalt, and manganese oxide NPs.

The dispersions of hydrophilic MNPs in polar solvents such as ethanol, methanol, THF, and DMF appeared to be quite stable over the time of observation (over a year). The solutions looks clear with no sign of scattered light from large NP aggregates, nor was there any precipitation of NPs observed. Figure 8 shows the hydrodynamic diameters of various hydrophilic MNPs in ethanol in which experimental data were obtained by a one year interval. The data suggest that the NP have remained well-separated and stable during that period of time.

To summarize a few merits of this ligand exchange reaction: First of all, the reactions were completed in just a few minutes, judging by the dark yet transparent appearance of the NP dispersion. Second, this method is a facile one-step reaction and high yield (>80%) of the hydrophilic NPs were obtained. Moreover, the resulting hydrophilic NPs can be dispersed in a wide range of solvents with excellent stability for at least 1 year, and the concentration could be as high as 100 mg/mL (10 wt %). Last but not the least, this method appears to be quite universal for the preparation of MNPs of different nature.

In Situ Synthesis of Aromatically Functionalized FePt Nanoparticles. In order to disperse NPs into solvents with low to intermediate polarity, we have synthesized FePt NPs

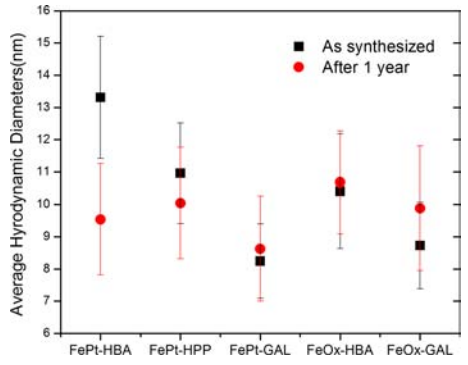

Figure 8. Average hydrodynamic diameters of exchanged MNPs obtained with Zetasizer for the as-synthesized hydrophilic NP dispersions in ethanol and the same dispersions after 1 year of sitting. Measurement were made without any sonication or filtration.

with aromatic ligands in a convenient one-pot fashion. Although this is not a ligand exchange reaction, it does provide the capability of NPs to be dispersed in less polar solvents (PI = 1.0−3.5) with minimum synthetic efforts. Aromatic rings in the ligand could not only provide sufficient protection due to their bulky size but also potentially facilitate NP dispersion in similar solvents such as toluene via potential $\pi-\pi$ interaction. The ligands we have chosen were biphenyl-4-carboxylic acid (BPCA), 2-naphthoic acid (2NA), and polystyrene (PS, M_n = 1K). The results are shown in Figure 9. FePt-BPCA and FePt-

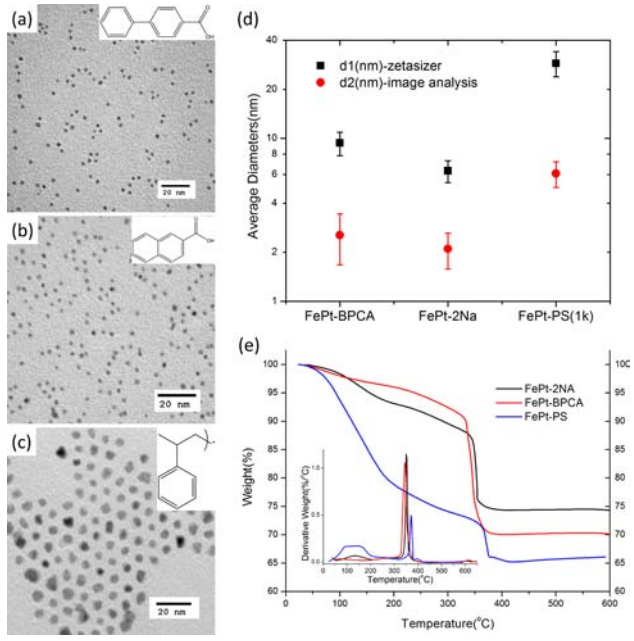

Figure 9. Transmission electron microscopy (TEM) images of FePt NPs with (a) biphenyl-4-carboxylic acid (BPCA), (b) 2-naphthoic acid (2NA), and (c) monocarboxy-terminated polystyrene (1K Da) as ligands. (d) Average diameters of NPs obtained from Zetasizer (DLS) and image analysis. (e) Thermogravimetric analysis (TGA) of the NPs.

2NA were very monodisperse with average core size of a little over 2 nm, whereas FePt-PS was about 6 nm. Noticed that the spacing between neighboring particles of FePt-PS was considerably larger than the other two due to the length of the extended polystyrene chain. For the same reason, the hydrodynamic diameter of FePt-PS was also considerably

dx.doi.org/10.1021/la404757q | Langmuir 2014, 30, 1514−1521

larger. It is worth noting that since the synthesis was a one-step reaction, the ligand distribution was extremely narrow as shown by the TGA data (Figure 9e). The areal ligand density (Σ) of FePt-BPCA (Σ = 8.6 ligand/nm^2), FePt-2NA (Σ = 6.6 ligand/nm^2), and FePt-PS (Σ = 5.0 ligand/nm^2) are all higher than that of hydrophobic FePt NPs with native alkyl chains. This is an indication of excellent ligand protection during the in situ synthesis of such NPs. This method covers the solvents of polarity index from low to intermediate, and the resulting NPs could be used to associate with conjugated soft materials through $\pi-\pi$ stacking interactions to form functional hybrid materials.

CONCLUSIONS

Within this report, we were able to demonstrate that hydrophilic NPs could be synthesized through simple one-step ligand exchange reactions with rationally chosen ligands. We have shown that small-molecule hydrophilic ligands have effectively replaced the original alkyl ligands on the NP surface within just a few minutes. The resulting hydrophilic NPs could be dispersed in a wide variety of polar organic solvents with superior stability over time. This method could be applied to many magnetic NPs regardless of their size and shape. One-pot synthesis of FePt NPs with aromatic ligands was also achieved to enable NPs to be dispersed in aromatic solvents. We believe that the synthetic routes reported here provide chances for magnetic NPs to be used in a broader field where NP dispersions in organic solvents were needed and will be beneficial to researchers of interest.

ASSOCIATED CONTENT

Supporting Information

Calculations of ligand coverage, histograms and DLS curves of MNPs, and proof of solution stability. This material is available free of charge via the Internet at http://pubs.acs.org.

AUTHOR INFORMATION

Corresponding Author

*E-mail watkins@polysci.umass.edu (J.J.W.).

Notes

The authors declare no competing financial interest.

ACKNOWLEDGMENTS

Funding for this research was provided by the National Science Foundation through the Center for Hierarchical Manufacturing (CHM, CMMI-1025020) at the UMass Amherst. X. Wang acknowledges Dr. Alec La Grow at the MacDiarmid Institute, Victoria University of Wellington, New Zealand, for the help with the synthesis of iron oxide nanoparticles.

REFERENCES

(1) Veiseh, O.; Sun, C.; Gunn, J.; Kohler, N.; Gabikian, P.; Lee, D.; Bhattarai, N.; Ellenbogen, R.; Sze, R.; Hallahan, A.; Olson, J.; Zhang, M. Optical and MRI Multifunctional Nanoprobe for Targeting Gliomas. *Nano Lett.* **2005**, *5* (6), 1003−1008.

(2) Huh, Y.-M.; Jun, Y.-w.; Song, H.-T.; Kim, S.; Choi, J.-s.; Lee, J.-H.; Yoon, S.; Kim, K.-S.; Shin, J.-S.; Suh, J.-S.; Cheon, J. In Vivo Magnetic Resonance Detection of Cancer by Using Multifunctional Magnetic Nanocrystals. *J. Am. Chem. Soc.* **2005**, *127* (35), 12387−12391.

(3) Cheong, S.; Ferguson, P.; Feindel, K. W.; Hermans, I. F.; Callaghan, P. T.; Meyer, C.; Slocombe, A.; Su, C.-H.; Cheng, F.-Y.; Yeh, C.-S.; Ingham, B.; Toney, M. F.; Tilley, R. D. Simple Synthesis and Functionalization of Iron Nanoparticles for Magnetic Resonance Imaging. *Angew. Chem., Int. Ed.* **2011**, *50* (18), 4206−4209.

(4) Jun, Y.-w.; Huh, Y.-M.; Choi, J.-s.; Lee, J.-H.; Song, H.-T.; KimKim; Yoon, S.; Kim, K.-S.; Shin, J.-S.; Suh, J.-S.; Cheon, J. Nanoscale Size Effect of Magnetic Nanocrystals and Their Utilization for Cancer Diagnosis via Magnetic Resonance Imaging. *J. Am. Chem. Soc.* **2005**, *127* (16), 5732−5733.

(5) Jeong, U.; Teng, X.; Wang, Y.; Yang, H.; Xia, Y. Superparamagnetic Colloids: Controlled Synthesis and Niche Applications. *Adv. Mater.* **2007**, *19* (1), 33−60.

(6) Lu, A.-H.; Salabas, E. L.; Schüth, F. Magnetic Nanoparticles: Synthesis, Protection, Functionalization, and Application. *Angew. Chem., Int. Ed.* **2007**, *46* (8), 1222−1244.

(7) Lee, I. S.; Lee, N.; Park, J.; Kim, B. H.; Yi, Y.-W.; Kim, T.; Kim, T. K.; Lee, I. H.; Paik, S. R.; Hyeon, T. Ni/NiO Core/Shell Nanoparticles for Selective Binding and Magnetic Separation of Histidine-Tagged Proteins. *J. Am. Chem. Soc.* **2006**, *128* (33), 10658−10659.

(8) Latham, A. H.; Freitas, R. S.; Schiffer, P.; Williams, M. E. Capillary Magnetic Field Flow Fractionation and Analysis of Magnetic Nanoparticles. *Anal. Chem.* **2005**, *77* (15), 5055−5062.

(9) Latham, A. H.; Tarpara, A. N.; Williams, M. E. Magnetic Field Switching of Nanoparticles between Orthogonal Microfluidic Channels. *Anal. Chem.* **2007**, *79* (15), 5746−5752.

(10) Pedro, T.; María del Puerto, M.; Sabino, V.-V.; Teresita, G.-C.; Carlos, J. S. The Preparation of Magnetic Nanoparticles for Applications in Biomedicine. *J. Phys. D: Appl. Phys.* **2003**, *36* (13), R182.

(11) Pankhurst, Q. A.; Connolly, J.; Jones, S. K.; Dobson, J. Applications of Magnetic Nanoparticles in Biomedicine. *J. Phys. D: Appl. Phys.* **2003**, *36* (13), R167.

(12) Catherine, C. B.; Adam, S. G. C. Functionalisation of Magnetic Nanoparticles for Applications in Biomedicine. *J. Phys. D: Appl. Phys.* **2003**, *36* (13), R198.

(13) Neuberger, T.; Schöpf, B.; Hofmann, H.; Hofmann, M.; von Rechenberg, B. Superparamagnetic Nanoparticles for Biomedical Applications: Possibilities and Limitations of a New Drug Delivery System. *J. Magn. Magn. Mater.* **2005**, *293* (1), 483−496.

(14) C.F. Chan, D.; B. Kirpotin, D.; A. Bunn, P., Jr. Synthesis and Evaluation of Colloidal Magnetic Iron Oxides for the Site-Specific Radio-Frequency-Induced Hyperthermia of Cancer. *J. Magn. Magn. Mater.* **1993**, *122* (1−3), 374−378.

(15) Sun, S.; Murray, C. B.; Weller, D.; Folks, L.; Moser, A. Monodisperse FePt Nanoparticles and Ferromagnetic FePt Nanocrystal Superlattices. *Science* **2000**, *287* (5460), 1989−1992.

(16) Sun, S. Recent Advances in Chemical Synthesis, Self-Assembly, and Applications of FePt Nanoparticles. *Adv. Mater.* **2006**, *18* (4), 393−403.

(17) Zeng, H.; Li, J.; Liu, J. P.; Wang, Z. L.; Sun, S. Exchange-Coupled Nanocomposite Magnets by Nanoparticle Self-Assembly. *Nature* **2002**, *420* (6914), 395−398.

(18) Mosallaei, H.; Sarabandi, K. Magneto-dielectrics in Electromagnetics: Concept and Applications. *IEEE Trans. Antennas Propag.* **2004**, *52* (6), 1558−1567.

(19) Lagarkov, A. N.; Rozanov, K. N. High-Frequency Behavior of Magnetic Composites. *J. Magn. Magn. Mater.* **2009**, *321* (14), 2082−2092.

(20) Hui, C.; Shen, C.; Yang, T.; Bao, L.; Tian, J.; Ding, H.; Li, C.; Gao, H.-J. Large-Scale Fe_3O_4 Nanoparticles Soluble in Water Synthesized by a Facile Method. *J. Phys. Chem. C* **2008**, *112* (30), 11336−11339.

(21) Salgueiriño-Maceira, V.; Liz-Marzán, L. M.; Farle, M. Water-Based Ferrofluids from Fe_xPt_{1-x} Nanoparticles Synthesized in Organic Media. *Langmuir* **2004**, *20* (16), 6946−6950.

(22) De la Presa, P.; Rueda, T.; Morales, M. P.; Hernando, A. Ligand Exchange in Gold-Coated FePt Nanoparticles. *IEEE Trans. Magn.* **2008**, *44* (11), 2816−2819.

(23) Gu, H.; Zheng, R.; Zhang, X.; Xu, B. Facile One-Pot Synthesis of Bifunctional Heterodimers of Nanoparticles: A Conjugate of

Quantum Dot and Magnetic Nanoparticles. *J. Am. Chem. Soc.* **2004**, *126* (18), 5664−5665.
(24) Chung, H. J.; Lee, H.; Bae, K. H.; Lee, Y.; Park, J.; Cho, S.-W.; Hwang, J. Y.; Park, H.; Langer, R.; Anderson, D.; Park, T. G. Facile Synthetic Route for Surface-Functionalized Magnetic Nanoparticles: Cell Labeling and Magnetic Resonance Imaging Studies. *ACS Nano* **2011**, *5* (6), 4329−4336.
(25) Ling, M. M.; Wang, K. Y.; Chung, T.-S. Highly Water-Soluble Magnetic Nanoparticles as Novel Draw Solutes in Forward Osmosis for Water Reuse. *Ind. Eng. Chem. Res.* **2010**, *49* (12), 5869−5876.
(26) Harris, L. A.; Goff, J. D.; Carmichael, A. Y.; Riffle, J. S.; Harburn, J. J.; St. Pierre, T. G.; Saunders, M. Magnetite Nanoparticle Dispersions Stabilized with Triblock Copolymers. *Chem. Mater.* **2003**, *15* (6), 1367−1377.
(27) Hong, R.; Fischer, N. O.; Emrick, T.; Rotello, V. M. Surface PEGylation and Ligand Exchange Chemistry of FePt Nanoparticles for Biological Applications. *Chem. Mater.* **2005**, *17* (18), 4617−4621.
(28) Keng, P. Y.; Shim, I.; Korth, B. D.; Douglas, J. F.; Pyun, J. Synthesis and Self-Assembly of Polymer-Coated Ferromagnetic Nanoparticles. *ACS Nano* **2007**, *1* (4), 279−292.
(29) Theppaleak, T.; Tumcharern, G.; Wichai, U.; Rutnakornpituk, M. Synthesis of Water Dispersible Magnetite Nanoparticles in the Presence of Hydrophilic Polymers. *Polym. Bull.* **2009**, *63* (1), 79−90.
(30) Lattuada, M.; Hatton, T. A. Functionalization of Monodisperse Magnetic Nanoparticles. *Langmuir* **2006**, *23* (4), 2158−2168.
(31) Kasture, M.; Singh, S.; Patel, P.; Joy, P. A.; Prabhune, A. A.; Ramana, C. V.; Prasad, B. L. V. Multiutility Sophorolipids as Nanoparticle Capping Agents: Synthesis of Stable and Water Dispersible Co Nanoparticles. *Langmuir* **2007**, *23* (23), 11409−11412.
(32) Gu, H.; Ho, P.-L.; Tsang, K. W. T.; Wang, L.; Xu, B. Using Biofunctional Magnetic Nanoparticles to Capture Vancomycin-Resistant Enterococci and Other Gram-Positive Bacteria at Ultralow Concentration. *J. Am. Chem. Soc.* **2003**, *125* (51), 15702−15703.
(33) Grubbs, R. B. Roles of Polymer Ligands in Nanoparticle Stabilization. *Polym. Rev.* **2007**, *47* (2), 197−215.
(34) Hyeon, T.; Lee, S. S.; Park, J.; Chung, Y.; Na, H. B. Synthesis of Highly Crystalline and Monodisperse Maghemite Nanocrystallites without a Size-Selection Process. *J. Am. Chem. Soc.* **2001**, *123* (51), 12798−12801.
(35) Kang, Y. S.; Risbud, S.; Rabolt, J. F.; Stroeve, P. Synthesis and Characterization of Nanometer-Size Fe_3O_4 and γ-Fe_2O_3 Particles. *Chem. Mater.* **1996**, *8* (9), 2209−2211.
(36) Sun, S.; Zeng, H. Size-Controlled Synthesis of Magnetite Nanoparticles. *J. Am. Chem. Soc.* **2002**, *124* (28), 8204−8205.
(37) Sun, S.; Zeng, H.; Robinson, D. B.; Raoux, S.; Rice, P. M.; Wang, S. X.; Li, G. Monodisperse MFe_2O_4 (M = Fe, Co, Mn) Nanoparticles. *J. Am. Chem. Soc.* **2003**, *126* (1), 273−279.
(38) Zeng, H.; Rice, P. M.; Wang, S. X.; Sun, S. Shape-Controlled Synthesis and Shape-Induced Texture of $MnFe_2O_4$ Nanoparticles. *J. Am. Chem. Soc.* **2004**, *126* (37), 11458−11459.
(39) Murray, C. B.; Sun, S.; Gaschler, W.; Doyle, H.; Betley, T. A.; Kagan, C. R. Colloidal synthesis of nanocrystals and nanocrystal superlattices. *IBM J. Res. Dev.* **2001**, *45* (1), 47−56.
(40) Nandwana, V.; Elkins, K. E.; Poudyal, N.; Chaubey, G. S.; Yano, K.; Liu, J. P. Size and Shape Control of Monodisperse FePt Nanoparticles. *J. Phys. Chem. C* **2007**, *111* (11), 4185−4189.
(41) Carenco, S.; Boissière, C. d.; Nicole, L.; Sanchez, C. m.; Le Floch, P.; Mézailles, N. Controlled Design of Size-Tunable Monodisperse Nickel Nanoparticles. *Chem. Mater.* **2010**, *22* (4), 1340−1349.
(42) Park, J.; Kang, E.; Son, S. U.; Park, H. M.; Lee, M. K.; Kim, J.; Kim, K. W.; Noh, H. J.; Park, J. H.; Bae, C. J.; Park, J. G.; Hyeon, T. Monodisperse Nanoparticles of Ni and NiO: Synthesis, Characterization, Self-Assembled Superlattices, and Catalytic Applications in the Suzuki Coupling Reaction. *Adv. Mater.* **2005**, *17* (4), 429−434.
(43) Latham, A. H.; Williams, M. E. Controlling Transport and Chemical Functionality of Magnetic Nanoparticles. *Acc. Chem. Res.* **2008**, *41* (3), 411−420.
(44) Fauconnier, N.; Pons, J. N.; Roger, J.; Bee, A. Thiolation of Maghemite Nanoparticles by Dimercaptosuccinic Acid. *J. Colloid Interface Sci.* **1997**, *194* (2), 427−433.
(45) Bagaria, H. G.; Ada, E. T.; Shamsuzzoha, M.; Nikles, D. E.; Johnson, D. T. Understanding Mercapto Ligand Exchange on the Surface of FePt Nanoparticles. *Langmuir* **2006**, *22* (18), 7732−7737.
(46) De Palma, R.; Peeters, S.; Van Bael, M. J.; Van den Rul, H.; Bonroy, K.; Laureyn, W.; Mullens, J.; Borghs, G.; Maes, G. Silane Ligand Exchange to Make Hydrophobic Superparamagnetic Nanoparticles Water-Dispersible. *Chem. Mater.* **2007**, *19* (7), 1821−1831.
(47) Xu, C.; Xu, K.; Gu, H.; Zhong, X.; Guo, Z.; Zheng, R.; Zhang, X.; Xu, B. Nitrilotriacetic Acid-Modified Magnetic Nanoparticles as a General Agent to Bind Histidine-Tagged Proteins. *J. Am. Chem. Soc.* **2004**, *126* (11), 3392−3393.
(48) Chen, Z. P.; Zhang, Y.; Zhang, S.; Xia, J. G.; Liu, J. W.; Xu, K.; Gu, N. Preparation and Characterization of Water-Soluble Monodisperse Magnetic Iron Oxide Nanoparticles via Surface Double-Exchange with DMSA. *Colloids Surf., A* **2008**, *316* (1−3), 210−216.
(49) Togashi, T.; Naka, T.; Asahina, S.; Sato, K.; Takami, S.; Adschiri, T. Surfactant-Assisted One-Pot Synthesis of Superparamagnetic Magnetite Nanoparticle Clusters with Tunable Cluster Size and Magnetic Field Sensitivity. *Dalton Trans.* **2011**, *40* (5), 1073−1078.
(50) Xu, C.; Xu, K.; Gu, H.; Zheng, R.; Liu, H.; Zhang, X.; Guo, Z.; Xu, B. Dopamine as a Robust Anchor to Immobilize Functional Molecules on the Iron Oxide Shell of Magnetic Nanoparticles. *J. Am. Chem. Soc.* **2004**, *126* (32), 9938−9939.
(51) Shultz, M. D.; Reveles, J. U.; Khanna, S. N.; Carpenter, E. E. Reactive Nature of Dopamine as a Surface Functionalization Agent in Iron Oxide Nanoparticles. *J. Am. Chem. Soc.* **2007**, *129* (9), 2482−2487.
(52) Peng, S.; Wang, C.; Xie, J.; Sun, S. Synthesis and Stabilization of Monodisperse Fe Nanoparticles. *J. Am. Chem. Soc.* **2006**, *128* (33), 10676−10677.
(53) Dong, A.; Ye, X.; Chen, J.; Kang, Y.; Gordon, T.; Kikkawa, J. M.; Murray, C. B. A Generalized Ligand-Exchange Strategy Enabling Sequential Surface Functionalization of Colloidal Nanocrystals. *J. Am. Chem. Soc.* **2010**, *133* (4), 998−1006.
(54) Rosen, E. L.; Buonsanti, R.; Llordes, A.; Sawvel, A. M.; Milliron, D. J.; Helms, B. A. Exceptionally Mild Reactive Stripping of Native Ligands from Nanocrystal Surfaces by Using Meerwein's Salt. *Angew. Chem., Int. Ed.* **2012**, *51* (3), 684−689.